Biomacromolecules

Open Access

pubs.acs.org/Biomac

Article

Co-Surfactant-Free Bioactive Protein Nanosheets for the Stabilization of Bioemulsions Enabling Adherent Cell Expansion

Alexandra Chrysanthou, Minerva Bosch-Fortea, and Julien E. Gautrot*

Cite This: *Biomacromolecules* 2023, 24, 4465−4477

Read Online

ACCESS | Metrics & More | Article Recommendations | Supporting Information

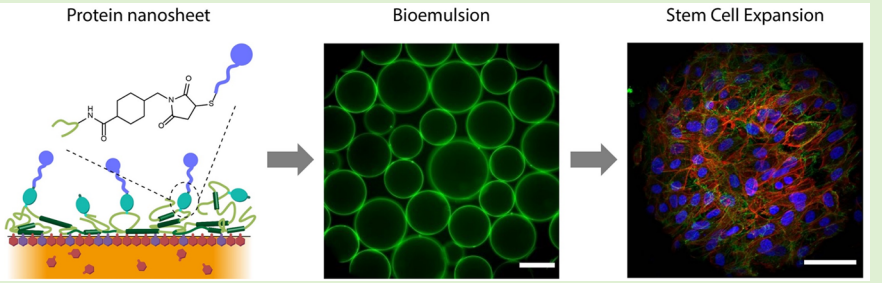

ABSTRACT: Bioemulsions are attractive platforms for the scalable expansion of adherent cells and stem cells. In these systems, cell adhesion is enabled by the assembly of protein nanosheets that display high interfacial shear moduli and elasticity. However, to date, most successful systems reported to support cell adhesion at liquid substrates have been based on coassemblies of protein and reactive cosurfactants, which limit the translation of bioemulsions. In this report, we describe the design of protein nanosheets based on two globular proteins, bovine serum albumin (BSA) and β-lactoglobulin (BLG), biofunctionalized with RGDSP peptides to enable cell adhesion. The interfacial mechanics of BSA and BLG assemblies at fluorinated liquid-water interfaces is studied by interfacial shear rheology, with and without cosurfactant acyl chloride. Conformational changes associated with globular protein assembly are studied by circular dichroism and protein densities at fluorinated interfaces are evaluated via surface plasmon resonance. Biofunctionalization mediated by sulfo-succinimidyl 4-(*N*-maleimidomethyl) cyclohexane-1-carboxylate (sulfo-SMCC) is studied by fluorescence microscopy. On the basis of the relatively high elasticities observed in the case of BLG nanosheets, even in the absence of cosurfactant, the adhesion and proliferation of mesenchymal stem cells and human embryonic kidney (HEK) cells on bioemulsions stabilized by RGD-functionalized protein nanosheets is studied. To account for the high cell spreading and proliferation observed at these interfaces, despite initial moderate interfacial elasticities, the deposition of fibronectin fibers at the surface of corresponding microdroplets is characterized by immunostaining and confocal microscopy. These results demonstrate the feasibility of achieving high cell proliferation on bioemulsions with protein nanosheets assembled without cosurfactants and establish strategies for rational design of scaffolding proteins enabling the stabilization of interfaces with strong shear mechanics and elasticity, as well as bioactive and cell adhesive properties. Such protein nanosheets and bioemulsions are proposed to enable the development of new generations of bioreactors for the scale up of cell manufacturing.

INTRODUCTION

Bioemulsions, emulsions that are bioactive and support the culture of adherent cells, are emerging as attractive solutions for the scale up of cell manufacturing.[1,2] Indeed, the absence of solid substrates or microcarriers is attractive to facilitate cell processing, reduce the contamination of cell products by microplastics and costs of culture consumables. Keese and Giaever first reported the culture of adherent cells at liquid interfaces, and identified the importance of surfactant molecules in mediating such process.[3,4] More recently, the importance of these surfactants, or co/pro-surfactants, together with the self-assembly of proteins, on the determination of mechanical properties of associated interfaces was identified. Co-assembly of proteins or polymers, such as poly(L-lysine) (PLL), with reactive surfactant acyl chlorides led to the stiffening of interfacial mechanics at corresponding liquid−liquid interfaces.[5,6] In turn, the resulting mechanically strong liquid−liquid interfaces are able to sustain shear forces developed by cells during their spreading and motility. In particular, the elastic properties of the protein assemblies at these interfaces, protein nanosheets, correlate with the proliferation of adherent stem cells, such as mesenchymal stem cells and keratinocytes.[5−7]

Special Issue: Polymers for Unmet Medical Challenges: Papers Presented at the Advanced Functional Polymers Medicine 2022 Conference

Received: October 31, 2022
Revised: January 3, 2023
Published: January 23, 2023

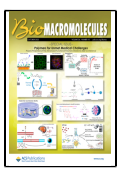

In this context, identifying assemblies that do not require co/pro-surfactants in order to strengthen interfacial mechanics is attractive, as it may enable faster translation of bioemulsions for stem cell manufacturing. Although a few systems have been proposed to date to promote stem cell adhesion and proliferation at liquid−liquid interfaces, they either rely on interfaces stabilized by undefined assemblies from serum proteins[8] or proteins that promote cell adhesion but do not readily stabilize emulsions, such as fibronectin.[9,10] Therefore, the identification of scaffolding proteins that display tensioactive properties enabling the stabilization of emulsion, confer strong interfacial mechanics and present bioactive and/or cell adhesive ligands enabling cell adhesion and proliferation remains elusive.

Recently, the modification of globulins such as albumins with charged residues was found to impact their assembly at liquid−liquid interfaces and resulting nanosheet mechanics.[11] These supercharged protein nanosheets enabled the simple adsorption of cell-adhesive proteins such as fibronectin and collagen, but the strengthening of their mechanical properties still required introduction of PFBC in order to sustain stem cell proliferation. This study demonstrated that simple protein modification may allow to modulate both nanosheet mechanics and bioactivity, however the identification of proteins and oils that enable the achievement of high interfacial elasticity in the absence of cosurfactant was not possible.

Globular proteins such as various globulins are attractive scaffold proteins for the design of nanosheets stabilizing bioemulsions as they can be sourced readily and are approved in a number of cases, at least for food applications, if not for use in therapeutics formulation. The functional properties of whey proteins are of substantial and growing importance to the food industry.[12] Proteins such as β-lactoglobulin are abundant, natural emulsifiers with relatively low cost. Associated food colloids are heterogeneous systems consisting of various kinds of particles and polymers. The nature and strength of interactions among them are the main determinants for the colloidal system properties that are highly influenced by the structure and composition of associated interfaces.[13]

Important physicochemical properties that define the ability of a protein to form and stabilize emulsions are size, solubility, hydrophobicity, charge and flexibility.[14] Strong viscoelastic films can provide electrostatic and steric stabilization, depending on the solvent conditions and the characteristics of the corresponding proteins. Flexible proteins such as caseins tend to form weaker viscoelastic films compared to globular compact proteins such as β-lactoglobulin, and may be more rapidly displaced by other surface active components.[14]

During the formation of protein nanosheets at liquid interfaces, proteins must first travel from the bulk phase toward the interface via diffusion. Once at the interface, protein molecules then unfold in order to expose hydrophobic amino acids to the surface. This partial denaturation of the protein will mediate the rearrangement of the hydrophobic amino acids to face the oil phase, while hydrophilic amino acids rearrange toward the aqueous phase. The reorientation and unfolding of the hydrophilic and hydrophobic residues leads to the minimization of thermodynamic energy.[15] The extent of conformational change depends on protein structure and the solvent conditions. Flexible proteins can rapidly adsorb at the interface, accelerating the reduction of interfacial tension without forming a dense and ordered packing layer. In contrast, globular proteins will pack at the interface, adsorbing at a slower rate but with higher order.[14] In addition, during the adsorption, disulfide bonds can be formed, further contributing to emulsion stability.[16]

β-lactoglobulin has a molecular weight of 18500 Da, contains five cysteins forming two disulfide linkages and is rich in β-sheet structures.[17,18] β-Lactoglobulin consists of three-turn α-helix and two β-sheets made by nine strands that are folded forming a hydrophobic calyx, classifying β-lactoglobulin into the lipocalin proteins family.[19] This formed calyx makes β-lactoglobulin able to bind to hydrophobic vitamins or lipids.[20] β-Lactoglobulin has an internal free sulfhydryl group which is only available as the protein adsorbs and partially unfolds.[12] During adsorption at the interface, β-lactoglobulin was proposed to form intermolecular β-sheet leading to the development of a strong protein viscoelastic nanosheet at the interface.[14] The high viscoelasticity of this film is further supported by intermolecular disulfide bonds due to the free thiol group present in the structure.[14] The high ordered packing thus created, together with intermolecular cross-links, makes the disruption of the film by other molecules such as surfactants extremely difficult.[14]

Therefore, β-lactoglobulin appears as an attractive scaffolding protein candidate for the design of viscoelastic protein nanosheets able to resist cell-mediated traction forces generated during spreading and proliferation. However, the lack of available integrin ligands able to initiate processes resulting in cell spreading requires further design of this protein. In addition, further combination with cosurfactant molecules such as acyl chlorides has not been studied.

Various approaches have been proposed to functionalize globular proteins with peptides. For example, bovine serum albumin (BSA) was functionalized with cyclic-RGD presenting free cysteines at the carboxylic end in order to mediate chemical coupling to maleimide residues introduced on the albumin through the heterobifunctional reagent sulfo-succinimidyl 4-(N-maleimidomethyl) cyclohexane-1-carboxylate (sulfo-SMCC).[21] This enabled to mediate cell adhesion to resulting albumin films that otherwise would block cell spreading.[21]

In this report, the viscoelastic behavior of BSA and β-lactoglobulin adsorbed at fluorinated oil interfaces are first investigated via interfacial shear rheology. The impact of the cosurfactant pentafluorobenzoyl chloride (PFBC) on this process is then studied. Conformational changes associated with the adsorption of these proteins at fluorinated oil interfaces are characterized via circular dichroism. The functionalization of resulting protein nanosheets with RGD cell adhesive peptides, using sulfo-SMCC as coupling agent, is then investigated. Finally, the proliferation of two adherent cell types, mesenchymal stem cells used in stem cell therapies, and HEK293 cells used for the expression of recombinant proteins, at the surface of bioemulsions stabilized by RGD-functionalized BSA and β-lactoglobulin is investigated. Cell adhesion and cytoskeleton assembly at the surface of nanosheet stabilized oil droplets are characterized and extra-cellular matrix deposition is studied.

MATERIALS AND METHODS

Materials and Chemicals. β-Lactoglobulin (>90%, from bovine milk), BSA (>98%, heat shock fraction), 1*H*,1*H*,2*H*,2*H*-perfluorodecanethiol (97%), and α,α,α-trifluorotoluene (99%) were obtained from Sigma-Aldrich Co. The reagent sulfo-succinimidyl 4-(*N*-maleimidomethyl) cyclohexane-l-carboxylate (sulfo-SMCC 22322)

https://doi.org/10.1021/acs.biomac.2c01289
Biomacromolecules 2023, 24, 4465−4477

and the SAMSA fluorescein, 5-((2-(and-3)-*S*-(acetylmercapto) succinoyl) amino) fluorescein, mixed isomers (A685) are purchased from Thermofischer Scientific. The fluorinated oil (Novec 7500; dodecafluoro-2-(trifluoromethyl)hexan-3-yl ethyl ether) is from ACOTA. SPR gold-coated chips were obtained from Ssens.

Preparation of Emulsions. For the emulsion generation 1 mL of fluorinated oil (Novec 7500, ACOTA) containing or not the fluorinated surfactant 2,3,4,5,6-pentafluorobenzoyl chloride at final concentration of 10 μg/mL and 2 mL protein solution (1 mg/mL in PBS) were added into a glass vial. The vial was shaken until the emulsion was created and further incubated for 1 h at room temperature. The upper liquid phase was aspirated and replaced with PBS 6 times.

Interfacial Shear Rheological Measurements. For the rheological measurements, a hybrid rheometer (DHR-3) from TA Instruments was used with a double wall ring (DWR) geometry and a Delrin trough with a circular channel. The DWR ring has a diamond-shaped cross section that enables the contact with the interface between two liquids to measure the properties. The ring has a radius of 34.5 mm with platinum−iridium wires of 1 mm thickness. The Derlin trough was filled with 19 mL of fluorinated oil (with or without surfactant) and using an axial force procedure. The ring was positioned at the interface by ensuring first contact, followed by lowering by 500 μm from this first contact point, to secure the correct position. After that, 15 mL of the PBS solution is placed on the top of the oil phase. Time sweeps were performed at a constant frequency of 0.1 Hz and temperature of 25 °C, with a displacement of 1.0×10^{-3} rad, to follow the protein adsorption at the interface. The protein solution (1 mg/mL) was added after 15 min in all cases. Before and after each time sweep, frequency sweeps (with constant displacement of 1.0×10^{-3} rad) were carried out to examine the frequency-dependent behavior of the interface and amplitude sweeps (with constant frequency of 0.1 Hz) to ensure that the chosen displacement was within the linear viscoelastic region.[6]

Surface Plasmon Resonance (SPR). SPR measurements were carried out on a BIACORE X from Biacore AB. SPR chips (SPR-Au 10 × 12 mm, Ssens) were plasma oxidized for 5 min and then incubated in a 5 mM ethanolic solution of 1*H*,1*H*,2*H*,2*H*-perfluorodecanethiol, overnight at room temperature. This created a model fluorinated monolayer mimicking the fluorophilic properties of Novec 7500. The chips were washed once with water, dried in an air stream and kept dry at room temperature prior to mounting (within a few minutes). Thereafter, the sensor chip was mounted on a plastic support frame and placed in a Biacore protective cassette. The maintenance sensor chip cassette was first placed into the sensor chip port and docked onto the Integrated μ-Fluidic Cartridge (IFC) flow block, prior to priming the system with ethanol. The sample sensor chip cassette was then docked and primed once with PBS. Once the sensor chip had been primed, the signal was allowed to stabilize to a stable baseline, and the protein solution (1 mg/mL in PBS) was loaded into the IFC sample loop with a micropipette (volume of 50 μL). The sample and buffer flow rates were kept at 10 μL/min throughout. After the injection finished, washing of the surface was carried out in running buffer (PBS) for 10 min. Washing of the surface was allowed to continue for 10 min prior to injection of sulfo-SMCC (at 2.0 mg/mL and volume of 50 μL), at a flow rate of 10 μL/min. The sensor chip was rinsed with buffer (PBS) for 10 min to wash off excess sulfo-SMCC solution, and data recording was allowed to continue for an additional 10 min. Lastly, RGD solutions (at 1.6 mg/mL and a volume of 50 μL), at a flow rate of 10 μL/min, were injected and allowed to adsorb for 10 min prior the final washing.

Circular Dichroism. For the circular dichroism measurements transparent emulsions were prepared. For matched refractive index emulsion oil mixture of α,α,α-trifluorotoluene and fluorinated oil were used in order to match the refractive index of water. A 1200 μL volume of fluorinated oil was mixed with 800 μL of α,α,α-trifluorotoluene. The oil mixture was mixed with 2 mL of protein solution at a concentration of 1 mg/mL. The emulsions were left at room temperature for 1 h, then washed 6 times with PB to remove excess free proteins and used fresh for measurements within 2 h. A 350 μL amount of emulsion was transferred to a sample cuvette for measurement in a Chirascan V100 CD spectrometer. Measurements were carried out at 25 °C. α,α,α-trifluorotoluene (99% - 547948) was purchased from Sigma-Aldrich Co. Measurements were smoothed using the Savitzky-Golay smooth filter with a script written in MATLAB and the secondary composition was estimated using the SELCON algorithm in Dichroweb. The concentration of proteins in emulsion samples was estimated based on the emulsion sizes measured (114 and 130 μm for BSA and BLG, respectively) and the surface densities of corresponding proteins determined from SPR measurements.

Evaluation of Emulsion Size. Emulsions were prepared as described above and stored at room temperature. The emulsion stability was monitored 7 days after the emulsion formation, using bright-field microscopy. A volume of 10 μL of emulsion was transferred to a 24-well plate, into 1 mL of PBS. Average microdroplet diameters were estimated from 100 droplets per condition.

Biofunctionalization of Protein Nanosheets. Proteins (BSA, β-lactoglobulin) were dissolved (at a concentration of 1 mg/mL) in PBS (pH 7.4). Emulsions were formed as stated above. The sulfo-SMCC was dissolved in (2 mg/mL) into 0.5 mL of distilled water under sonication for 2 min and then added to the emulsion for 1 h at room temperature. The upper liquid phase was aspirated and replaced with PBS six times to remove the excess of the sulfo-SMCC. For the SAMSA fluorescein activation, SAMSA-fluorescein (10 mg/mL) was dissolved into 0.1 M NaOH and incubated at room temperature for 15 min to remove acetyl protecting groups. Fourteen μL of 6 M HCl were added to 0.2 mL of 0.5 M sodium phosphate at pH 7. To each emulsion, 40 μL of dye solution were added and the upper liquid was replaced again with PBS six times to remove the excess of the dye. After the dye reaction, the emulsion was washed with PBS six times. Samples of each emulsion were transferred to a microwell plate for imaging.

Mesenchymal Stem Cell Culture and Seeding. Mesenchymal stem cells (P3−6, Promocell) were cultured in mesenchymal stem cell growth medium 2 (PromoCell). For proliferation assays, MSCs were harvested with accutase solution containing 0.5 mM EDTA (PromoCell) and incubated at 37 °C for 5 min. Cells were resuspended in medium at a ratio of 1:1, centrifuged for 5 min at 1200 rpm, counted, and resuspended in MSC medium at a desired density. Cells were allowed to adhere and proliferate on these substrates/emulsions in an incubator (37 °C and 5% CO_2) for different times points (day three, five and seven of culture), prior the staining and imaging. For the cell spreading assay and matrix deposition assay, cells were seeded at concentration of 10,000 cells per well (for seeding directly on plastic substrates) or 50000 cells per well (for seeding on emulsions, to match the seeding density per surface area). For passaging, cells were reseeded at a density of 300000 cells per T75 flask.

Human Embryonic Kidney Cells Culture and Seeding. Human embryonic kidney (HEK293) cells were cultured in DMEM (Thermofisher Scientific) containing 10% fetal bovine serum (FBS, Labtech) and 1% penicillin-streptavidin (5000 U/mL). Cells were harvested with trypsin (0.25%) and versene solutions (Thermo Fisher Scientific, 0.2 g/L EDTA Na_4 in phosphate buffered saline) at a ratio of 1/9. Cells were resuspended in DMEM at a ratio 1:1 and centrifuged for 5 min at 1200 rpm. HEK293T cells were counted and resuspended in DMEM and seeded onto the substrates at a density of 5000 cells per well (for seeding directly on plastic substrates) or 25000 cells per well (for seeding on emulsions, to match the seeding density per surface area). For passaging, cells were reseeded at a density of 200000 cell per T75 flask.

Metabolic Assay − CCK8. Cell Counting Kit 8 (CCK-8) assay (Sigma-Aldrich -96992) was used to assess cell viability according to manufacturer's instructions. Briefly, the CCK-8 reagent was added at each sample and at the standard curve samples (for MSCs − 10k, 25k, 50k, 75k, 100k, and 200k, and for HEK293T − 5k, 20k, 50k, 100k, 200k, and 300k) and incubated for 3 h in the incubator at 37 °C. A volume of 100 μL (all samples were triplicates) was taken from each sample, and the absorbance was measured at 450 nm at days one,

https://doi.org/10.1021/acs.biomac.2c01289
Biomacromolecules 2023, 24, 4465−4477

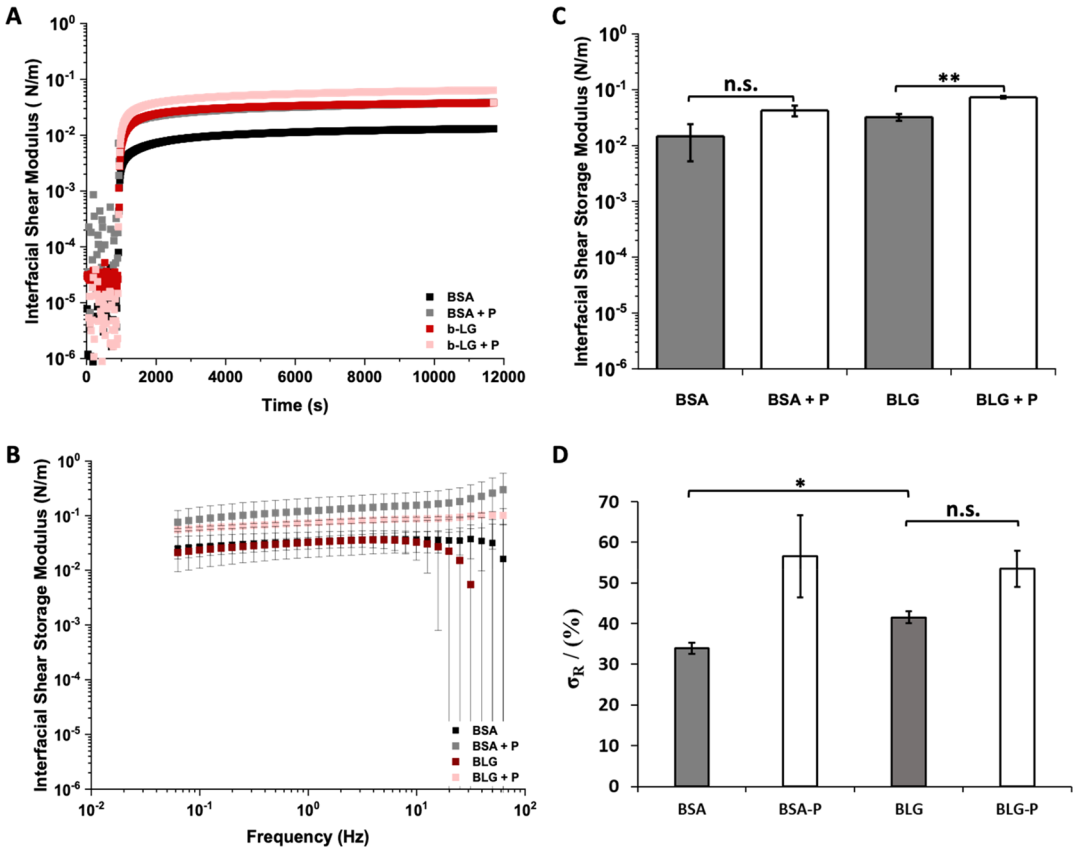

Figure 1. (A) Evolution of interfacial storage moduli during the adsorption of BSA and β-lactoglobulin, with and without PFBC (10 μg/mL with respect to the oil phase). (B) Frequency sweep of the protein nanosheets and (C) the corresponding interfacial storage modulus at an oscillating amplitude of 10^{-4} rad and frequency of 1 Hz. (D) Residual interfacial elasticities (stress retentions, σ_R, %) extracted from the fits of stress relaxation experiments at 0.5% strain (see Supporting Information, Figure S2 for representative examples of traces).

three, five, and seven for HEK293T and at days three, five, and seven for MSCs.

Immuno-Fluorescence Staining and Antibodies. Samples (emulsions) were washed (dilution and aspiration, followed by addition of solutions) once with PBS and fixed with 4% paraformaldehyde (Sigma-Aldrich; 8% for samples in Ibidi well plates) for 10 min at room temperature. Thereafter, samples were washed three times with PBS and permeabilized with 0.2% Triton X-100 (Sigma-Aldrich; 0.4% for samples in Ibidi well plates) for 5 min at room temperature. After washing with PBS (three times), samples were blocked for 1 h in 3% BSA. The blocking buffer was partly removed from the samples, not allowing them to be exposed to air, and the samples were incubated with primary antibodies at 4 °C overnight. Samples were washed six times with PBS and incubated for 1 h with the secondary antibodies (phalloidin (Sigma - P1951), 1:500; DAPI, 1:1000; vinculin (Sigma - V9264), 1:1000; fibronectin (Sigma - F3648), 1:500; Ki67 (Abcam - ab15580), 1:500) in blocking buffer (3% BSA in PBS). After washing with PBS (six times), samples were transferred to Ibidi wells for imaging.

Immuno-Fluorescence Microscopy and Data Analysis. Fluorescence microscopy images were acquired with a Zeiss 710 Confocal Microscope using a 63× and 20× objective to image the MSCs and HEK293T.

Statistical Analysis. Statistical analysis was carried out using OriginPro 9 through one-way ANOVA with Tukey test for posthoc analysis. Significance was determined by $^*P < 0.05$, $^{**}P < 0.01$, $^{***}P < 0.001$ and n.s., nonsignificant. A full summary of the statistical analysis is provided in the Supporting Information.

RESULTS AND DISCUSSION

The formation of protein nanosheets based on bovine serum albumin (BSA) and β-lactoglobulin (BLG) at oil−water interfaces was first characterized using interfacial rheology (Figure 1). Focus was placed on interfaces formed with the fluorinated oil Novec 7500 due to its broad application in a range of microdroplet microfluidic technologies and its low cytotoxicity.[22,23] Upon injection of BSA and BLG solutions, the interfacial shear storage modulus of the corresponding liquid−liquid interfaces increased by 2−3 orders of magnitude, as shown in the Figure 1A. This is in agreement with previous reports, indicating that albumin readily adsorbs to a range of oil−water interfaces, forming a highly viscoelastic interface with interfacial dilatational storage[24−27] moduli in the range of 20−60 mN/m, depending on the technique used. The variation in values measured likely reflects variations in batch and source of the proteins used, but also the type of interfacial rheology applied. In particular, techniques relying on droplet shape analysis result in moduli that depend on surface tension, as well as the shear moduli of the corresponding interfaces, rather than purely on shear properties.[28] Indeed, surface tensions are comparable to dilatational interfacial shear moduli of many protein-stabilized liquid−liquid or liquid−air interfaces[28,29] and contribute in significant levels to interfacial mechanics, in addition to Coulombic interactions, assessed by dilatational rheology and via AFM indentations.[30] β-Lactoglobulin led to the formation of interfaces with comparable interfacial storage moduli compared to BSA

https://doi.org/10.1021/acs.biomac.2c01289
Biomacromolecules 2023, 24, 4465−4477

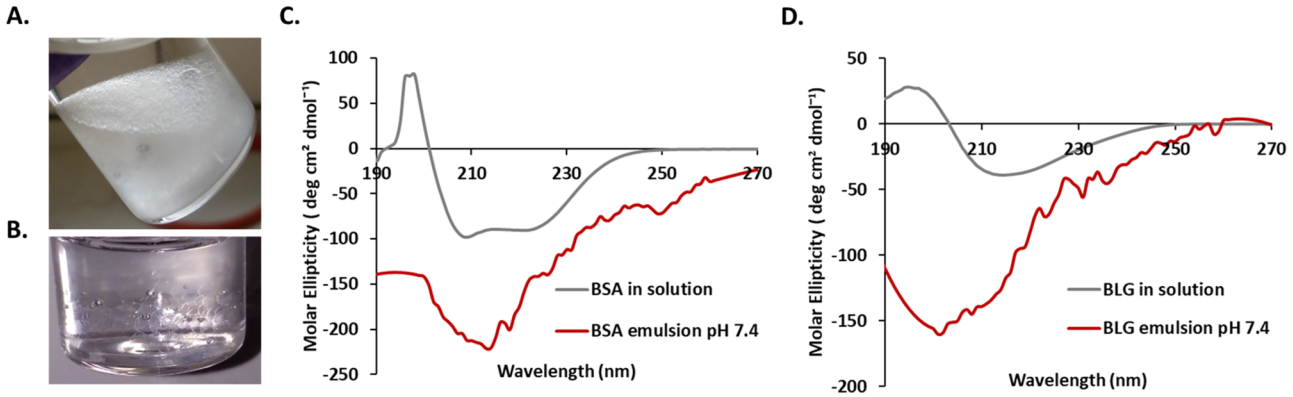

Figure 2. (A) Representative image of a Novec 7500−water emulsion. (B) Refractive index matched emulsion made with a mixture of Novec 7500 and trifluorotoluene. CD spectra of (C) BLG in solution (at concentration 1 mg/mL) and adsorbed in an oil−water interface (after removing excess free protein) and (D) BSA in solution (at concentration 1 mg/mL) and adsorbed at the oil−water interface (after removing excess free protein).

(Figure 1A−C). These data are in good agreement with the relatively fast adsorption of β-lactoglobulin and BSA at other hydrophobic liquid interfaces, while adsorption to more polar hydrophobic liquid was retarded and led to weaker interfacial mechanics.[29,31,32]

The interfacial shear moduli of the generated interfaces was found to be moderately dependent on oscillating frequencies, indicating the formation of viscoelastic interfaces (Figure 1B). In addition, frequency sweeps further confirmed that β-lactoglobulin formed interfaces with equivalent interfacial shear moduli to BSA. These results were further confirmed by comparison of interfacial storage and loss moduli data (Figure 1C and Supporting Information, Figure S1). The interfacial loss moduli of BSA and BLG were both nearly 1 order of magnitude lower than corresponding interfacial storage moduli. However, while the interfacial shear storage modulus of BLG was found to be modestly higher than that of BSA (not significant), its interfacial loss modulus was not. To further investigate viscoelastic properties of BSA and BLG interfaces, interfacial stress relaxation experiments were carried out using recently established protocols[7] (Supporting Information, Figures S2 and S3). Significant levels of elasticity (high elastic stress retention, σ_R) were observed in BLG-stabilized interfaces, compared to BSA (Figure 1D). Therefore, these data indicate that while BSA and BLG interfaces display comparable interfacial storage moduli, their elasticity differs, suggesting more extended cross-linked networks are obtained for BLG.

The addition of cosurfactant molecules was previously found to significantly affect interfacial mechanics, in particular viscoelastic profiles.[5,7,33] Therefore, the impact of the introduction of the pro-surfactant pentafluorobenzoyl chloride (PFBC) was studied next (Figure 1A). Acyl chlorides such as PFBC are described as cosurfactants, rather than surfactants, as they display moderate tensioactive properties and instead couple covalently to proteins or polymers to promote their adsorption or modulate the mechanics of the resulting interfaces.[5,7,33] Both BSA and BLG interfaces were found to display higher storage and loss moduli in the presence of PFBC (Figure 1A−C and Supporting Information, Figure S1), indicating that the coupling of these hydrophobic residues enhanced physical cross-links within the protein layer. Indeed, a wider range of hydrophobic acyl chloride was previously reported to induce nanosheet strengthening through the formation of hydrophobic cross-links (noncovalent cross-links mediated by van der Waals forces between hydrophobic residues).[7] Changes in interfacial viscoelastic behavior were particularly striking, with enhancement in elastic stress from 34 and 42% for BSA and BLG interfaces (respectively) to 57 and 54% for BSA and BLG nanosheets formed in the presence of PFBC (Figure 1D and Supporting Information, Figure S2). Considering the higher elasticity observed for BLG interfaces in the absence of PFBC, the magnitude of the change in stress retention observed in relaxation experiments was found to be stronger for BSA nanosheets. This difference may also stem from the significantly higher number of lysine residues (near 60 per molecule) in BSA compared to β-lactoglobulin (only 15 lysines). As the amines of lysines are proposed to couple to acyl chlorides (although other residues such as serines may also contribute to reactivity), the presence of higher lysine densities may enhance physical cross-linking and associated elasticity of BSA nanosheets.

The formation of highly elastic protein nanosheets, in the absence of a cosurfactant, is attractive for enabling a faster translation of these assemblies due to the lack of validation of these molecules, including PFBC, by regulatory bodies. Therefore, BLG is an attractive candidate for the stabilization of liquid−liquid interfaces and strengthening of their mechanical properties in the absence of PFBC or other cosurfactants, to enable cell adhesion and proliferation on liquid substrates such as microdroplets. Although the impact of BLG on surface tension, the stabilization of emulsions, and interfacial shear mechanics is well established,[34−36] the origin of its strengthening of interfacial shear mechanics is not completely understood.

To explore the mechanism associated with β-lactoglobulin strengthening of interfacial shear mechanics, the conformation of BSA and BLG was investigated in solution and at liquid−liquid interfaces. β-Lactoglobulin consists of 33% β-sheet structures, which is significantly higher than the β-sheet content of BSA (10%).[37−39] This high percentage of β-sheet confers to BLG, a β-structure that is more rigid than other α-helix-dominated or disordered proteins.[40−42] The higher rigidity of β-sheet-rich proteins was studied by boson peak frequency analysis by Perticalori et al., concluding that the increased stiffness of β-structured proteins compare to that of α-structured proteins.[43] Upon adsorption at hydrophobic liquid interfaces, rearrangement of the protein structure may

https://doi.org/10.1021/acs.biomac.2c01289
Biomacromolecules 2023, 24, 4465−4477

significantly impact the interfacial mechanics by enabling exposure of hydrophobic residues that may provide intermolecular cross-links.[31,44] In addition to structural changes, free thiol groups may contribute to the further cross-linking of associated protein networks and modulate interfacial mechanics or stabilize emulsions.[12,45,46]

To study conformation changes in BSA and BLG upon assembly at liquid−liquid interfaces, circular dichroism (CD) measurements were carried out with emulsions. In order to enable such measurements, mixtures of Novec 7500 and α,α,α-trifluorotoluene (1.5:1 ratio) were used (refractive indexes of Novec 7500 and of α,α,α-trifluorotoluene are 1.29 and 1.41, respectively),[47] with the refractive index matching that of PBS buffer. This afforded clear emulsions that enabled CD measurements (Figure 2A). The CD spectra of free BSA and BLG solutions was in good agreement with their expected structure and reports from the literature[48,49] (Figure 2B/C). BLG, in solution, was found to exhibit strong β-sheet components and associated profile, with the characteristic positive maximum at 195 nm, the negative maximum at 218 nm and the zero crossings at 207 and 250 nm.[49] To quantify the conformational contribution associated with such spectra, the SELCON algorithm from Dichroweb was used.[50] The calculated composition of BLG structures in solution was found to be 17% α-helix, 41% β-sheet and the remaining corresponding to disordered and β-turns structures, consistent with previous results and the estimated secondary structure (Table 1).[49] In contrast, in solution, BSA displayed strong α-helical components, with a positive peak at 195 nm, a double negative peak at 210 and 222 nm, and a zero crossing at 205 nm (Figure 2C). This corresponded to an α-helix content of 72%, with no significant β-sheet contribution, and the rest accounted by β-turns and disordered domains, in good agreement with the expected structure of BSA and previously reported CD data.[18,38]

Table 1. Secondary Structure Composition of BSA and BLG in Solution and at Interfaces Calculated Using the SELCON Algorithm in DichroWeb, Based on Circular Dichroism Data

	secondary structure (%)			
	helix	sheet	turns	unordered
BSA in solution	72	0	10	18
BSA in emulsion	25	13	14	48
BLG in solution	17	42	26	15
BLG in emulsion	17	31	12	39

Significant changes in CD spectra were observed in emulsions (Figure 2B,C). The α-helix contribution of BSA reduced to only 26%, whereas some β-sheet contribution occurred (13%), and the disordered contribution increased to 48%. In contrast, the α-helix composition of BLG remained unchanged, and its β-sheet component increased to 31%, with an increase of disordered domains (from 15 to 38%). Hence, CD spectra indicate a significant unfolding of BSA and BLG at fluorinated oil interfaces with a predominant disordered structure. Similar trends were observed for BSA and myoglobin adsorbed at the hexadecane/water interface, showing an increase in the disordered structure (17 to 27% and 13 to 29%, respectively).[18] It should be noted that molar ellipticities were based on the starting concentration of protein in solution (in the aqueous phase) and that concentrations at the interfaces of emulsions were not corrected, despite the aqueous phase having been washed and exchanged for protein-free buffer.

These results are in general agreement with previous reports in which FT-IR spectra indicated high β-sheet content for BLG in solution (45%), with minor α-helix content (7%).[51] Upon adsorption to triacylglycerol (TAG), β-sheet components were found to reduce modestly to 25% while, α-helix and random coil contributions increased from 7% to 25% and from 20% to 27%, respectively.[52] Similarly, β-sheet content of BLG adsorbed at diacylglycerol (DAG)−water interfaces was reduced from 45% to 35%, although a moderate level compared to BLG at TAG interfaces, while the α-helix component increased from 7% to 20%.[52] It was suggested that the enhanced unfolding at DAG−water interfaces, compared to TAG−water, results from the associated reduced surface coverage. Such a decrease in surface coverage was proposed to originate from the higher polarity of the DAG compared to TAG.[51] Indeed, surface coverage correlated with the polarity of TAG and *n*-tetradecane.[51] These changes were also comparable to those reported by Zhai et al., indicating a partial loss in β-sheet and an increase in α-helix composition and disordered domains.[40,53] Other studies have also proposed the conversion of α-helical-rich proteins such as BSA, lysozyme, and myoglobin to β-sheet components upon adsorption to oil−water interfaces.[18]

Therefore, overall, our results suggest a significant change in protein structure upon assembly at fluorinated oil interfaces. Therefore, it is possible that intermolecular interactions between residues exposed upon such conformational rearrangement may underlie the physical cross-linking of associated protein nanosheets and the level of elasticity observed, even in the absence of PFBC coupling. However, more extensive cross-linking requires additional residues, introduced through PFBC molecules. The high hydrophobicity of the fluorinated oil studied may also contribute to enhance protein unfolding and surface coverage and associated protein entanglement, facilitating cross-linking. However, the precise nature of the conformational changes taking place upon protein unfolding at liquid−liquid interfaces is difficult to establish, and the exact contribution of unfolding to entanglement and cross-linking, for example via α-helix/α-helix or β-sheet interactions, is difficult to establish. Finally, the oligomerization state of BLG, known to be modulated by the pH of associated solutions, may also impact interfacial assembly and mechanics, although at the pH of the present study, BLG was reported to be predominantly dimeric.[54−57].

Despite these encouraging interfacial mechanical properties, BSA and BLG remain inherently globular proteins playing roles in molecular transport and lipid stabilization in physiological fluids,[58−60] with little relevance to ECM signaling and the promotion of cell adhesion. To confer cell adhesion to these scaffold proteins, we coupled an RGD peptide to the surface of protein nanosheet-stabilized droplets. The heterobifunctional coupling agent sulfo-SMCC was allowed to tether to nanosheets, prior to washing of excess and incubation in cysteine-terminated peptides displaying the cell adhesive ligand RGDSP.[21] To determine the success of this tethering strategy, the thiolated dye 5-((S-(acetylmercapto)succinoyl amino fluorescein (SAMSA) was coupled instead of peptides, prior to quantification via fluorescence microscopy (Figure 3). Michael-addition of SAMSA was carried out to sulfo-SMCC activated droplets stabilized by BSA and BLG nanosheets. This

https://doi.org/10.1021/acs.biomac.2c01289
Biomacromolecules 2023, 24, 4465−4477

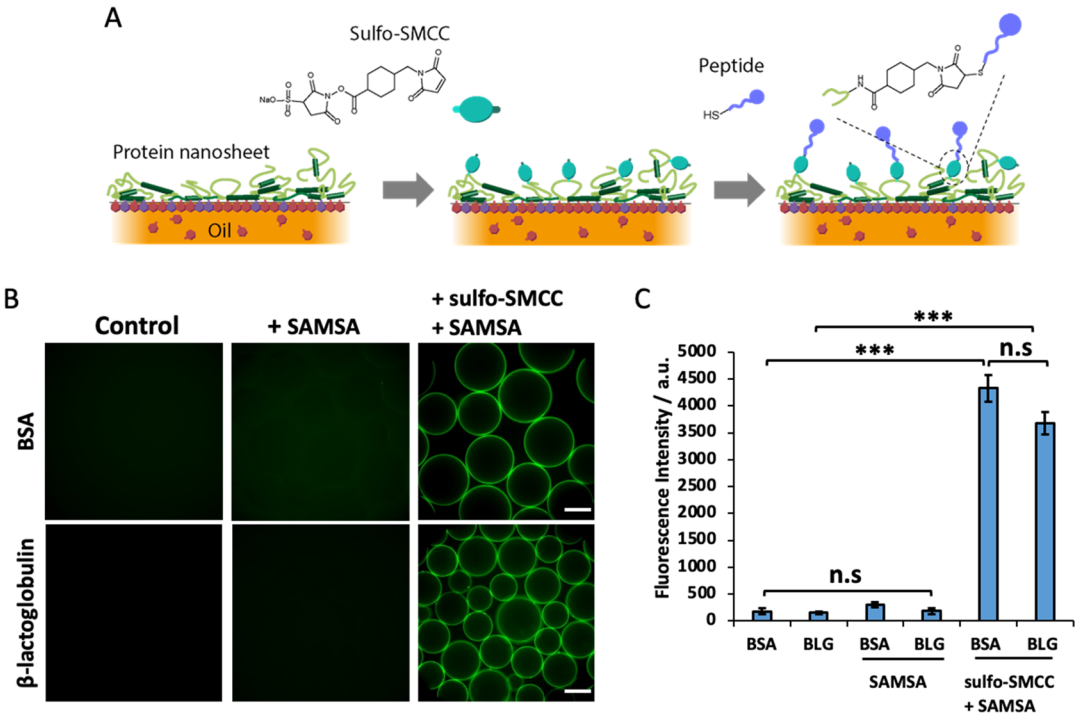

Figure 3. (A) Schematic representation of the functionalization protocol. (B) Epifluorescence microscopy images of BSA or BLG emulsions functionalized with SAMSA fluorescein (green, A685) with or without sulfo-SMCC. (C) Mean fluorescence intensity of the coupled SAMSA. Scale bars, 100 μm. Error bars are s.e.m.; n = 3.

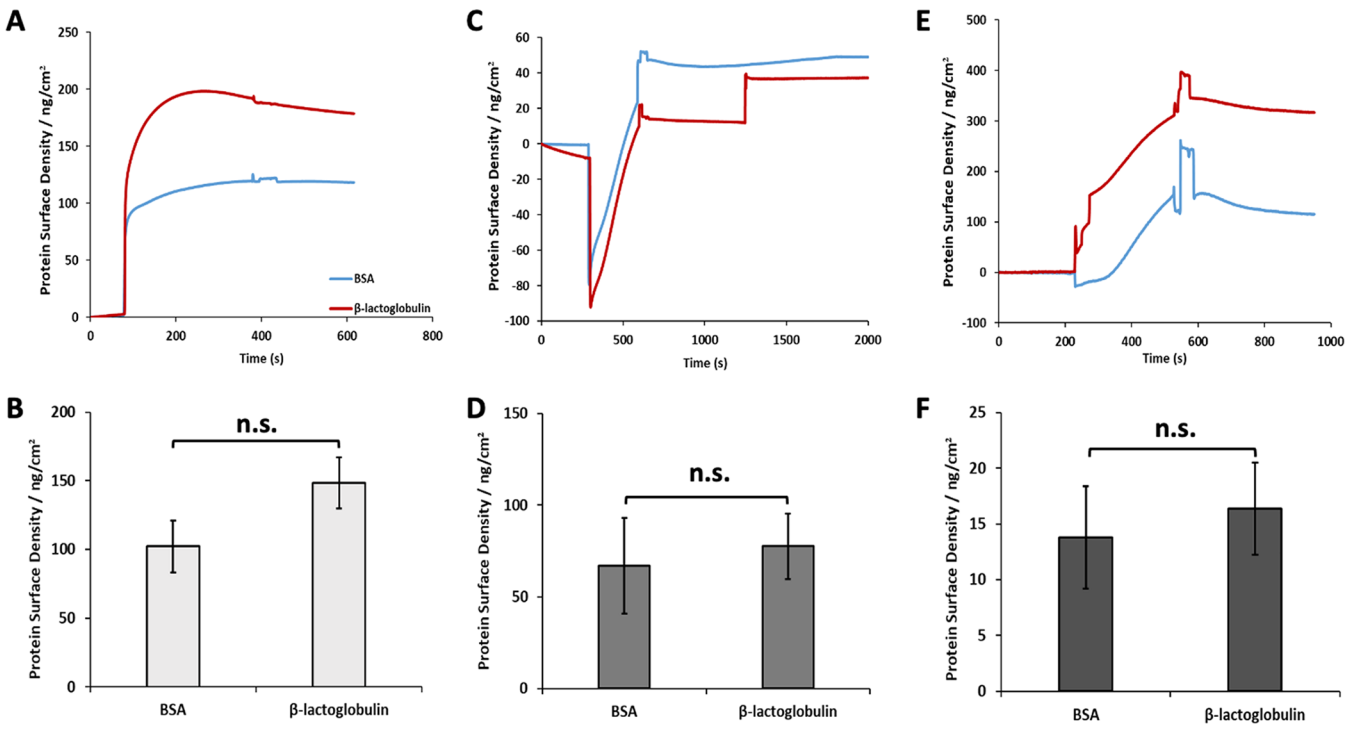

Figure 4. (A) Representative surface plasmon resonance traces displaying the adsorption of BSA and BLG to perfluorodecanethiol monolayers modeling fluorinated oil interfaces. (B) Corresponding quantification of resulting protein surface densities. (C) SPR quantification of sulfo-SMCC coupling at the surface of BSA and BLG layers. (D) Corresponding calculated additional mass. (E) SPR quantification of RGD coupling at the surface of sulfo-SMCC layers. (F) Corresponding peptide surface densities. Error bars are s.e.m.; n = 3.

resulted in homogeneous levels of functionalization, over the droplet surface and throughout the droplet population (Figure 3). Quantification of the fluorescence indicated overall comparable levels of functionalization on BSA and BLG nanosheets, with excellent retention of emulsion stability (note that the emulsions studied were generated by vortexing and inherently polydisperse in size). The control groups, maleimide-free, did not display any significant functionalization

https://doi.org/10.1021/acs.biomac.2c01289
Biomacromolecules 2023, 24, 4465−4477

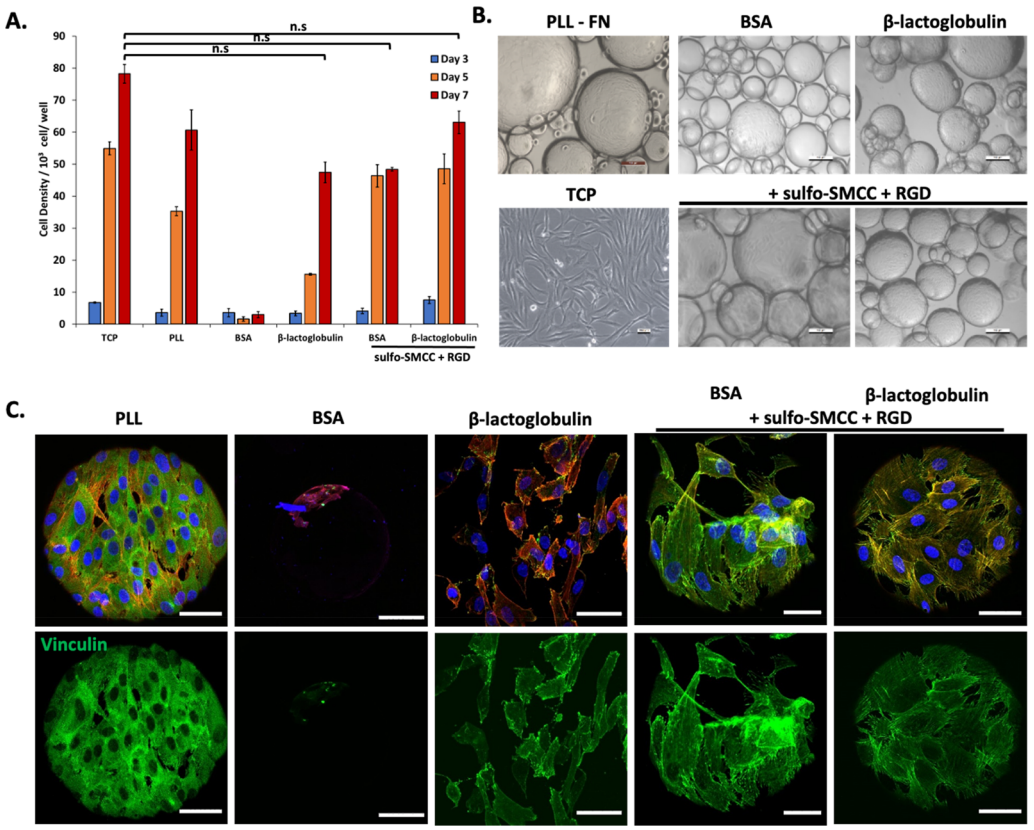

Figure 5. (A) Proliferation of mesenchymal stem cells (MSC) at the surface of bioemulsions stabilized PLL, BSA, or BLG nanosheets, with or without RGD functionalization. Based on metabolic assay. Comparison with tissue culture plastic (TCP) control. (B) Corresponding bright field images of MSCs cultured for 7 days. (C) Confocal images of MSCs cultured for 7 days on corresponding bioemulsions and controls (blue, DAPI; red, phalloidin; green, vinculin). Scale bars are 100 μm (bright field) and 50 μm (confocal). Error bars are s.e.m.; n = 3.

or conjugation with SAMSA, demonstrating that the coupling is maleimide-specific and enabling the potential control of ligand density. The lack of fluorescence from pristine nanosheet-stabilized emulsions (without sulfo-SMCC or SAMSA) also confirmed the lack of autofluorescence from adsorbed proteins. Taken together, these results demonstrate the capability of this approach to directly functionalize a variety of protein nanosheet-stabilized microdroplets, a flexible approach to systematically combine peptide formulations.

To further investigate the functionalization process, surface plasmon resonance (SPR) was used to characterize associated successive steps (Figure 4). To better capture the structure of nanosheets formed at fluorinated liquid interfaces, SPR chips were functionalized with a monolayer of perfluorinated thiol. This is potentially leading to adsorption mechanisms that will differ from adsorption to Novec 7500, but would better capture representative adsorption/functionalization profiles to fluorinated oils than direct adsorption to gold surfaces (of the SPR chips). It is important to note that adsorption to monolayers may differ from that at liquid−liquid interfaces (in particular Novec 7500 is not a simple perfluorinated alkane, but rather a perfluorinated ether) and SPR does not enable the introduction of cosurfactants such as PFBC. The adsorption of BSA and β-lactoglobulin was found to be comparable (Figure 4B,C and Supporting Information, Figure S4), although perhaps associated with slightly thicker or denser BLG assemblies. The adsorption levels measured for BSA (120 ng/cm^2) and BLG (180 ng/cm^2) were not statistically different and corresponded to protein submonolayers in both cases. Indeed, perfectly packed monolayers of BSA would give rise to densities ranging from 190 to 630 ng/cm^2 (depending on the orientation and assuming no unfolding; taking dimensions of 141 × 42 × 42 nm), whereas BLG would give rise to densities near 230 ng/cm^2 (assuming a closely packed sphere of 3.6 nm diameter). Therefore, the adsorption levels observed suggest either submonolayer formation, or significant unfolding. In turn, coupling of sulfo-SMCC was associated with changes in surface densities of 70 and 80 ng/cm^2 for BSA and BLG respectively, presumably corresponding to the mass increase associated with coupling and potential further changes in protein conformation (see Figure 4C,D). Finally, peptide coupling was associated with further increase in mass densities of 14 and 16 ng/cm^2 (for BSA and BLG, respectively; comparable for both proteins; see Figure 4E,F). The kinetics at which the reaction took place was slower, reflecting the lower concentration of peptides compared to sulfo-SMCC, and despite the higher molar mass of the cell adhesive peptide selected. However, with a molar mass of 805 g/mol, this level of adsorption remains associated with a degree of coupling of 12 and 2 peptides per protein (BSA and BLG, respectively) and peptide surface densities of 0.10 and 0.12 peptides/nm^2. Therefore, the distance between each peptide for both bioactive protein nanosheet interfaces is below 10 nm, clearly under the threshold beyond which cells are able to sense reductions in adhesive ligand densities.[61] Therefore, the maleimide-based coupling of RGD peptides to BSA and BLG nanosheets was found to be well within the densities that

https://doi.org/10.1021/acs.biomac.2c01289
Biomacromolecules 2023, 24, 4465−4477

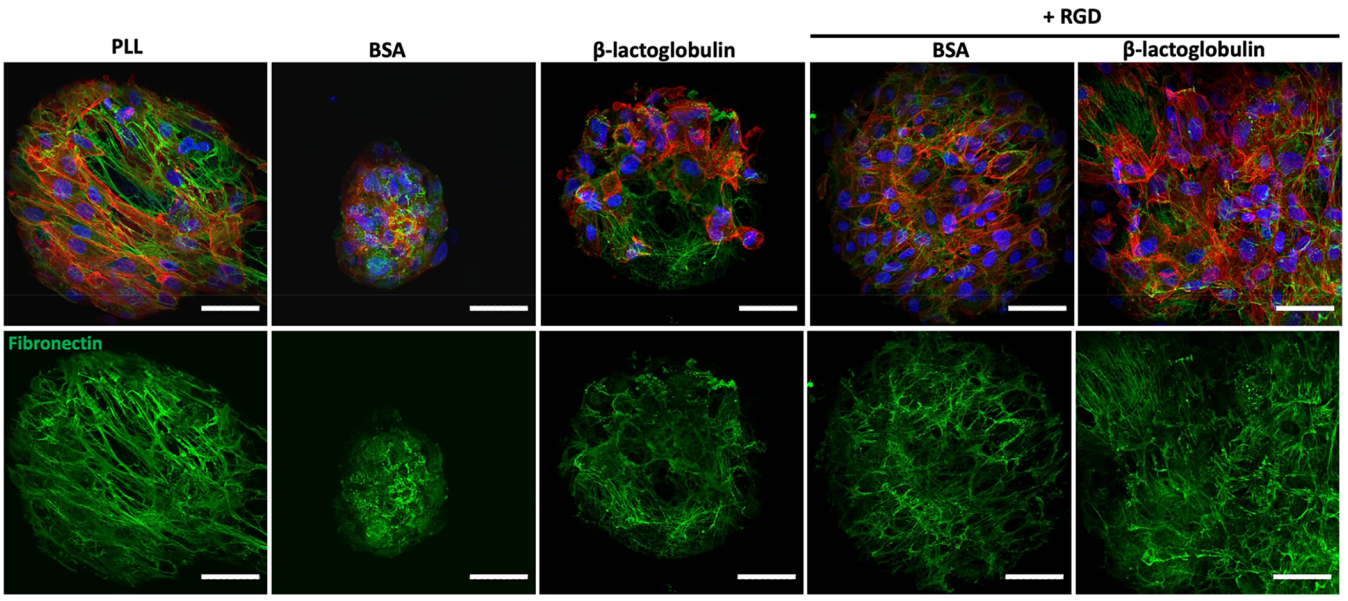

Figure 6. Confocal images of MSCs cultured for 7 days on bioemulsions stabilized by protein nanosheets. Characterization of fibronectin deposition (blue, DAPI; red, phalloidin; green, fibronectin;). Scale bars are 50 μm (confocal). Error bars are s.e.m.; n = 3.

are considered suitable to enable rapid cell adhesion and spreading.

Having demonstrated the suitable biofunctionalization of protein nanosheets with cell-adhesive ligands, the culture of mesenchymal stem cells (MSCs) at these interfaces was next investigated. MSCs were cultured at the surface of oil droplets stabilized by RGD-functionalized protein nanosheets. The study of MSC culture at the surface of PFBC-reinforced nanosheets was not examined as such system had already be explored in the context of BSA[6] and one of the aims of the present work was to establish protein candidates supporting cell culture in the absence of cosurfactants. As a comparison, in addition to tissue culture plastic (TCP) controls, poly(L-lysine) (PLL) nanosheet-stabilized emulsions were also investigated, as the expansion of MSCs to such interfaces has previously been reported and characterized extensively.[5] After 7 days of culture, MSCs were found to have proliferated significantly at the surface of BSA and BLG nanosheet-stabilized emulsions functionalized with RGD peptides, to levels comparable to those observed on TCP and PLL-stabilized microdroplets (Figure 5A). Cell colonies were found to cover droplets relatively homogeneously, with high droplet occupancies (Figure 5B and Supporting Information, Figure S5). At day 7, cell densities were slightly higher on BLG/RGD-emulsions than BSA/RGD-emulsions. Surprisingly, although very few cells were found on BSA-emulsions, cell densities at the surface of BLG-emulsions were comparable to those observed on BSA/RGD-emulsions and only slightly below those of BLG/RGD-emulsions. As no cell-adhesive ligand has been reported within the structure of BLG, to the best of our knowledge, these results suggest instead that matrix adsorption to BLG dominates this behavior. This may be underpinned by the presence of many cysteines and disulfide bonds within the structure of BLG. In addition to other nonspecific interactions with unfolded exposed residues, this may promote the nonspecific adsorption of ECM proteins that may then mediate cell adhesion. Interestingly, although BSA nanosheets were found to display relatively low elasticities, cell adhesion, and proliferation at these interfaces was found to be relatively high, without supplementation with PFBC. This may suggest further maturation of the mechanical properties of corresponding nanosheets, perhaps in response to matrix adsorption.

To further investigate cell adhesion to nanosheet-stabilized emulsions, the formation of focal adhesions and cytoskeleton assembly were investigated (Figure 5C). Although quantification was not carried out, due to the difficulty of imaging such curved interfaces at high resolution, with suspended droplets, images clearly indicated the formation of focal adhesions and establishment of a mature cytoskeleton on BSA/RGD and BLG/RGD bioemulsions, comparable to the phenotype of MSCs spreading to PLL-stabilized emulsions. In contrast, the few cells that were found to spread on BSA-emulsions were relatively rounded. However, in agreement with the high proliferation of MSCs at BLG-emulsions, despite the lack of RGD functionalization, cells were found to form focal adhesions and assemble a cytoskeleton on BLG nanosheets, although their spreading seemed slightly reduced compared to BLG/RGD nanosheets. Therefore, these results indicate that the expansion of MSCs at the surface of BSA/RGD and BLG/RGD-stabilized bioemulsions is mediated by cell adhesive ligands and regulated by the classic acto-myosin machinery, as was previously observed on fibronectin coated PLL-stabilized liquid−liquid interfaces.[5] These results are consistent with the high interfacial moduli and relatively high elasticities observed for these nanosheets, in particular BLG, as well as high ligand densities achieved, as both of these surface properties are classically associated with the regulation of cell adhesion, spreading, and proliferation at various interfaces.[62−64]

A surprising aspect of these results is that cell adhesion and spreading was found to be excellent on both BSA/RGD and BLG/RGD nanosheets, despite the moderate elasticities measured for both interfaces, in the absence of PFBC (Figure 1), as the ability of liquid−liquid interfaces to store strain energy and resist deformation was found to be highly correlated with adherent cell expansion at liquid−liquid interfaces.[65] To further explore some of the possible mechanisms via which cell adhesion to droplets stabilized by relatively viscous nanosheets (low interfacial elasticity), matrix

https://doi.org/10.1021/acs.biomac.2c01289
Biomacromolecules 2023, 24, 4465−4477

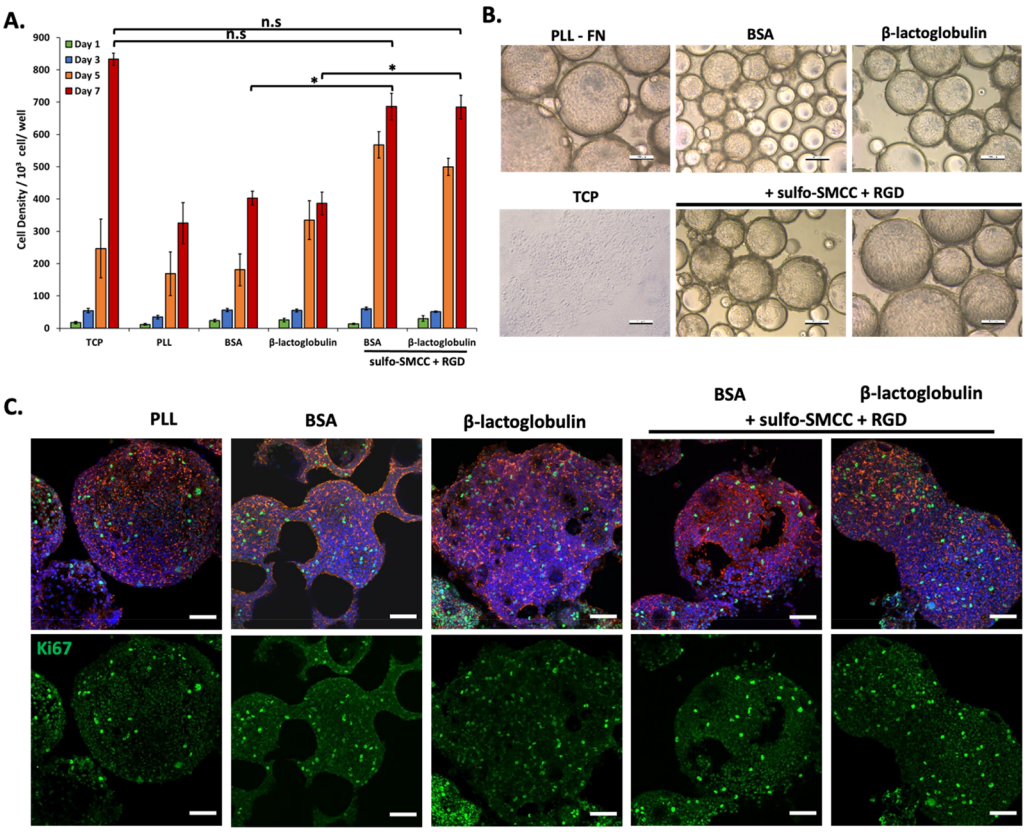

Figure 7. (A) Proliferation of Human embryonic kidney cells (HEK293T) at the surface of bioemulsions stabilized PLL, BSA, or BLG nanosheets, with or without RGD functionalization. Based on metabolic assay. Comparison with tissue culture plastic (TCP) control. (B) Corresponding bright field images of MSCs cultured for 7 days. (C) Confocal images of MSCs cultured for 7 days on corresponding bioemulsions and controls (blue, DAPI; red, phalloidin; green, Ki67). Scale bars are 100 μm (bright field) and 50 μm (confocal). Error bars are s.e.m.; n = 3.

deposition was investigated (Figure 6). MSCs culture for 7 days on bioemulsions deposited fibronectin fibers that covered the surface of droplets and formed relatively dense networks. Interestingly, this was also the case at the surface of BLG-emulsions, with matrix deposition also visible in gaps within cell colonies, suggesting that matrix remodeling underpins at least some of the adhesion and proliferation of MSCs at these interfaces. In addition, on the few BSA-stabilized emulsions that supported MSC adhesion, some fibronectin assembly was clearly visible, suggesting that such phenomenon might contribute to the proliferation of these rare colonies. This may be associated with the direct assembly of fibronectin (or other ECM proteins) at hydrophobic liquid interfaces, as this process was found to be sufficient to support the adhesion and proliferation of some stem cells (although not on emulsions, given the poor tensioactive properties of fibronectin).[10] Alternatively, it may be that fibronectin (or other ECM molecules) are able to adsorb to assembled denatured BSA.

Finally, the culture of human embryonic kidney cells (HEK293T), often used for the expression of recombinant proteins by mammalian cells,[66,67] was explored at the surface of bioemulsions, to demonstrate the potential of these platforms for the production of biotherapeutics and recombinant proteins. Cell densities were characterized at days 1, 3, 5, and 7 (Figure 7). Interestingly, all conditions were found to support relatively high cell densities, compared to those observed for MSCs. However, HEK293 proliferation was particularly strong at the surface of BSA/RGD and BLG/RGD emulsions, comparable to that observed on TCP. In non-functionalized BSA and BLG emulsions, although relatively high proliferation was observed, many droplets could be seen to be devoid of colonies and HEK293 were found to form aggregates that seem weakly adhered to neighboring droplets. This may be associated with the capacity of HEK293 cells to sustain moderate proliferation in suspension, or in weak adhesive states.[68] To confirm the high proliferation observed on these various interfaces, Ki67 staining, a marker reflecting cell cycling, was investigated (Figure 7C). This indicated clear levels of proliferation on all emulsions, supporting the bright field imaging and cell density quantification data.

CONCLUSIONS

In this study, the possibility to grow cells on microdroplets stabilized by defined scaffold proteins, in the absence of further cosurfactant assembly, was demonstrated. Protein nanosheet assembly is found to be associated with significant denaturation and conformational rearrangement, depending on the protein type. Such conformational changes may be the basis for the formation of relatively elastic networks interconnecting assembled proteins and underpinned by reassociation between rearranged residues, although such processes remains to be demonstrated formally. However, with β-lactoglobulin too, as previously shown with albumins,[33] the mechanics of these networks can further mature in the presence of PFBC. Overall, supramolecular interactions can drive the formation of quasi-2D elastic protein networks. Although it is important to stress that these supramolecular processes are unlikely to be well-defined and are expected to lack specificity, instead relying on

https://doi.org/10.1021/acs.biomac.2c01289
Biomacromolecules 2023, 24, 4465−4477

disordered unfolding, entanglement and likely underpinning weak physical cross-linking. Covalent strategies to further mature and further tune the mechanics of these networks are expected to bring further control to these interfaces, as was recently demonstrated in the case of simply exposure to DTT, likely promoting disulfide bond formation.[69]

In addition, this study demonstrates a straightforward strategy for the biofunctionalization of preassembled scaffold proteins and corresponding emulsions, with cell adhesive peptides. Sulfo-SMCC mediated coupling can be readily applied to a variety of other scaffold proteins and a broad range of peptides sequences can be selectively coupled to these residues through Michael additions. Finally, this study demonstrates that the resulting bioactive nanosheets support the adhesion and proliferation of MSCs and HEK293 cells at the surface of corresponding bioemulsions. β-lactoglobulin-stabilized bioemulsions are found to perform better in this respect, as a result of improved elasticity, compared to BSA-stabilized emulsion. However, clear adhesion remains observed to BSA/RGD, despite slightly lower elasticity, and even unfunctionalized BLG-stabilized interfaces supported some cell proliferation. This may be associated with matrix deposition and remodeling at these interfaces, as cells are able to deposit significant levels of fibronectin fibers at corresponding interfaces. Overall, this study indicates that replacing cosurfactant molecules such as PFBC and achieving bioactivity with readily available scaffold proteins typically encountered in food processing and stem cell technologies is possible.

■ ASSOCIATED CONTENT

Supporting Information

The Supporting Information is available free of charge at https://pubs.acs.org/doi/10.1021/acs.biomac.2c01289.

Additional interfacial shear rheology data, fluorescence microscopy images of emulsions, and tables summarizing the results of statistical analysis (PDF)

■ AUTHOR INFORMATION

Corresponding Author

Julien E. Gautrot − *Institute of Bioengineering and School of Engineering and Materials Science, Queen Mary, University of London, London E1 4NS, United Kingdom;* orcid.org/0000-0002-1614-2578; Email: j.gautrot@qmul.ac.uk

Authors

Alexandra Chrysanthou − *Institute of Bioengineering and School of Engineering and Materials Science, Queen Mary, University of London, London E1 4NS, United Kingdom*

Minerva Bosch-Fortea − *Institute of Bioengineering and School of Engineering and Materials Science, Queen Mary, University of London, London E1 4NS, United Kingdom*

Complete contact information is available at: https://pubs.acs.org/10.1021/acs.biomac.2c01289

Notes

The authors declare the following competing financial interest(s): J.G. is the Chief Scientific Officer of Liquibio Limited, a registered limited company developing emulsion technologies for the life sciences.

■ ACKNOWLEDGMENTS

The authors are grateful for experimental support and training from Dr. Dexu Kong. Funding for this work from the European Research Council (ProLiCell, 772462; ProBioFac, 966740) and from a Cyprus Scholarship (IKYK, 841C18) is gratefully acknowledged.

■ REFERENCES

(1) Peng, L.; Gautrot, J. E. Long Term Expansion Profile of Mesenchymal Stromal Cells at Protein Nanosheet-Stabilised Bio-emulsions for next Generation Cell Culture Microcarriers. *Mater. Today Bio* **2021**, *12*, 100159.

(2) Bellani, C. F.; Ajeian, J.; Duffy, L.; Miotto, M.; Groenewegen, L.; Connon, C. J. Scale-Up Technologies for the Manufacture of Adherent Cells. *Front. Nutr.* **2020**, *7*, 575146.

(3) Keese, C. R.; Giaever, I. Cell Growth on Liquid Interfaces: Role of Surface Active Compounds. *Proc. Natl. Acad. Sci. U. S. A.* **1983**, *80* (18), 5622−5626.

(4) Keese, C. R.; Giaever, I. Cell Growth on Liquid Microcarriers. *Science* **1983**, *219* (4591), 1448−1449.

(5) Kong, D.; Peng, L.; Di Cio, S.; Novak, P.; Gautrot, J. E. Stem Cell Expansion and Fate Decision on Liquid Substrates Are Regulated by Self-Assembled Nanosheets. *ACS Nano* **2018**, *12* (9), 9206−9213.

(6) Kong, D.; Megone, W.; Nguyen, K. D. Q.; Di Cio, S.; Ramstedt, M.; Gautrot, J. E. Protein Nanosheet Mechanics Controls Cell Adhesion and Expansion on Low-Viscosity Liquids. *Nano Lett.* **2018**, *18* (3), 1946−1951.

(7) Kong, D.; Peng, L.; Bosch-Fortea, M.; Chrysanthou, A.; Alexis, C. V. J.-M.; Matellan, C.; Zarbakhsh, A.; Mastroianni, G.; del Rio Hernandez, A.; Gautrot, J. E. Impact of the Multiscale Viscoelasticity of Quasi-2D Self-Assembled Protein Networks on Stem Cell Expansion at Liquid Interfaces. *Biomaterials* **2022**, *284*, 121494.

(8) Hanga, M. P.; Nienow, A. W.; Murasiewicz, H.; Pacek, A. W.; Hewitt, C. J.; Coopman, K. Expansion of Human Mesenchymal Stem/Stromal Cells on Temporary Liquid Microcarriers. *J. Chem. Technol. Biotechnol.* **2021**, *96* (4), 930−940.

(9) Minami, K.; Mori, T.; Nakanishi, W.; Shigi, N.; Nakanishi, J.; Hill, J. P.; Komiyama, M.; Ariga, K. Suppression of Myogenic Differentiation of Mammalian Cells Caused by Fluidity of a Liquid−Liquid Interface. *ACS Appl. Mater. Interfaces* **2017**, *9* (36), 30553−30560.

(10) Jia, X.; Minami, K.; Uto, K.; Chang, A. C.; Hill, J. P.; Nakanishi, J.; Ariga, K. Adaptive Liquid Interfacially Assembled Protein Nanosheets for Guiding Mesenchymal Stem Cell Fate. *Adv. Mater.* **2020**, *32* (4), 1905942.

(11) Chrysanthou, A.; Kanso, H.; Zhong, W.; Shang, L.; Gautrot, J. E. Supercharged Protein Nanosheets for Cell Expansion on Bioemulsions. *bioRxiv 2022.06.21.497058* **2022**, na.

(12) Dickinson, E.; Hong, S.-T. Surface Coverage of. Beta.-Lactoglobulin at the Oil-Water Interface: Influence of Protein Heat Treatment and Various Emulsifiers. *J. Agric. Food Chem.* **1994**, *42* (8), 1602−1606.

(13) Dickinson, E. Colloid Science of Mixed Ingredients. *Soft Matter* **2006**, *2* (8), 642.

(14) Wilde, P. J. Emulsions and Nanoemulsions Using Dairy Ingredients. *Dairy-Derived Ingredients*; Woodhead Publishing, 2009; 539−564. DOI: 10.1533/9781845697198.3.539.

(15) Lam, R. S. H.; Nickerson, M. T. Food Proteins: A Review on Their Emulsifying Properties Using a Structure−Function Approach. *Food Chem.* **2013**, *141* (2), 975−984.

(16) Tcholakova, S.; Denkov, N. D.; Sidzhakova, D.; Campbell, B. Effect of Thermal Treatment, Ionic Strength, and PH on the Short-Term and Long-Term Coalescence Stability of β-Lactoglobulin Emulsions. *Langmuir* **2006**, *22* (14), 6042−6052.

(17) Singh, H. Protein Interactions and Functionality of Milk Protein Products. *Dairy-Derived Ingredients*; Woodhead Publishing, 2009; 644−674. DOI: 10.1533/9781845697198.3.644.

(18) Day, L.; Zhai, J.; Xu, M.; Jones, N. C.; Hoffmann, S. V.; Wooster, T. J. Conformational Changes of Globular Proteins Adsorbed at Oil-in-Water Emulsion Interfaces Examined by Synchrotron Radiation Circular Dichroism. *Food Hydrocoll.* **2014**, *34*, 78−87.
(19) Singh, H. Aspects of Milk-Protein-Stabilised Emulsions. *Food Hydrocoll.* **2011**, *25* (8), 1938−1944.
(20) Le Maux, S.; Giblin, L.; Croguennec, T.; Bouhallab, S.; Brodkorb, A. β-Lactoglobulin as a Molecular Carrier of Linoleate: Characterization and Effects on Intestinal Epithelial Cells in Vitro. *J. Agric. Food Chem.* **2012**, *60* (37), 9476−9483.
(21) Delforge, D.; Gillon, B.; Art, M.; Dewelle, J.; Raes, M.; Remacle, J. Design of a Synthetic Adhesion Protein by Grafting RGD Tailed Cyclic Peptides on Bovine Serum Albumin. *Lett. Pept. Sci.* **1998**, *5* (2−3), 87−91.
(22) Theberge, A. B.; Courtois, F.; Schaerli, Y.; Fischlechner, M.; Abell, C.; Hollfelder, F.; Huck, W. T. S. Microdroplets in Microfluidics: An Evolving Platform for Discoveries in Chemistry and Biology. *Angew. Chem., Int. Ed.* **2010**, *49* (34), 5846−5868.
(23) Kaminski, T. S.; Scheler, O.; Garstecki, P. Droplet Microfluidics for Microbiology: Techniques, Applications and Challenges. *Lab. Chip* **2016**, *16* (12), 2168−2187.
(24) Baldursdottir, S. G.; Fullerton, M. S.; Nielsen, S. H.; Jorgensen, L. Adsorption of Proteins at the Oil/Water Interface—Observation of Protein Adsorption by Interfacial Shear Stress Measurements. *Colloids Surf. B Biointerfaces* **2010**, *79* (1), 41−46.
(25) Freer, E. M.; Yim, K. S.; Fuller, G. G.; Radke, C. J. Interfacial Rheology of Globular and Flexible Proteins at the Hexadecane/Water Interface: Comparison of Shear and Dilatation Deformation. *J. Phys. Chem. B* **2004**, *108* (12), 3835−3844.
(26) Freer, E. M.; Yim, K. S.; Fuller, G. G.; Radke, C. J. Shear and Dilatational Relaxation Mechanisms of Globular and Flexible Proteins at the Hexadecane/Water Interface. *Langmuir* **2004**, *20* (23), 10159−10167.
(27) Alexandrov, N.; Marinova, K. G.; Danov, K. D.; Ivanov, I. B. Surface Dilatational Rheology Measurements for Oil/Water Systems with Viscous Oils. *J. Colloid Interface Sci.* **2009**, *339* (2), 545−550.
(28) Benjamins, J.; Lyklema, J.; Lucassen-Reynders, E. H. Compression/Expansion Rheology of Oil/Water Interfaces with Adsorbed Proteins. Comparison with the Air/Water Surface. *Langmuir* **2006**, *22* (14), 6181−6188.
(29) Lucassen-Reynders, E. H.; Benjamins, J.; Fainerman, V. B. Dilational Rheology of Protein Films Adsorbed at Fluid Interfaces. *Curr. Opin. Colloid Interface Sci.* **2010**, *15* (4), 264−270.
(30) Megone, W.; Kong, D.; Peng, L.; Gautrot, J. E. Extreme Reversal in Mechanical Anisotropy in Liquid-Liquid Interfaces Reinforced with Self-Assembled Protein Nanosheets. *J. Colloid Interface Sci.* **2021**, *594*, 650−657.
(31) Bergfreund, J.; Bertsch, P.; Kuster, S.; Fischer, P. Effect of Oil Hydrophobicity on the Adsorption and Rheology of β-Lactoglobulin at Oil−Water Interfaces. *Langmuir* **2018**, *34* (16), 4929−4936.
(32) Jung, J.-M.; Gunes, D. Z.; Mezzenga, R. Interfacial Activity and Interfacial Shear Rheology of Native β-Lactoglobulin Monomers and Their Heat-Induced Fibers. *Langmuir* **2010**, *26* (19), 15366−15375.
(33) Kong, D.; Megone, W.; Nguyen, K. D. Q.; Di Cio, S.; Ramstedt, M.; Gautrot, J. E. Protein Nanosheet Mechanics Controls Cell Adhesion and Expansion on Low-Viscosity Liquids. *Nano Lett.* **2018**, *18* (3), 1946−1951.
(34) Jung, J.-M.; Gunes, D. Z.; Mezzenga, R. Interfacial Activity and Interfacial Shear Rheology of Native β-Lactoglobulin Monomers and Their Heat-Induced Fibers. *Langmuir* **2010**, *26* (19), 15366−15375.
(35) Bergfreund, J.; Bertsch, P.; Kuster, S.; Fischer, P. Effect of Oil Hydrophobicity on the Adsorption and Rheology of β-Lactoglobulin at Oil−Water Interfaces. *Langmuir* **2018**, *34* (16), 4929−4936.
(36) Lucassen-Reynders, E. H.; Benjamins, J.; Fainerman, V. B. Dilational Rheology of Protein Films Adsorbed at Fluid Interfaces. *Curr. Opin. Colloid Interface Sci.* **2010**, *15* (4), 264−270.
(37) Yu, J.; Chen, Y.; Xiong, L.; Zhang, X.; Zheng, Y. Conductance Changes in Bovine Serum Albumin Caused by Drug-Binding Triggered Structural Transitions. *Materials* **2019**, *12* (7), 1022.
(38) Murayama, K.; Tomida, M. Heat-Induced Secondary Structure and Conformation Change of Bovine Serum Albumin Investigated by Fourier Transform Infrared Spectroscopy. *Biochemistry* **2004**, *43* (36), 11526−11532.
(39) Zhai, J.; Miles, A. J.; Pattenden, L. K.; Lee, T.-H.; Augustin, M. A.; Wallace, B. A.; Aguilar, M.-I.; Wooster, T. J. Changes in β-Lactoglobulin Conformation at the Oil/Water Interface of Emulsions Studied by Synchrotron Radiation Circular Dichroism Spectroscopy. *Biomacromolecules* **2010**, *11* (8), 2136−2142.
(40) Zhai, J.; Miles, A. J.; Pattenden, L. K.; Lee, T.-H.; Augustin, M. A.; Wallace, B. A.; Aguilar, M.-I.; Wooster, T. J. Changes in β-Lactoglobulin Conformation at the Oil/Water Interface of Emulsions Studied by Synchrotron Radiation Circular Dichroism Spectroscopy. *Biomacromolecules* **2010**, *11* (8), 2136−2142.
(41) Perticaroli, S.; Nickels, J. D.; Ehlers, G.; O'Neill, H.; Zhang, Q.; Sokolov, A. P. Secondary Structure and Rigidity in Model Proteins. *Soft Matter* **2013**, *9* (40), 9548.
(42) Perticaroli, S.; Nickels, J. D.; Ehlers, G.; Sokolov, A. P. Rigidity, Secondary Structure, and the Universality of the Boson Peak in Proteins. *Biophys. J.* **2014**, *106* (12), 2667−2674.
(43) Perticaroli, S.; Nickels, J. D.; Ehlers, G.; O'Neill, H.; Zhang, Q.; Sokolov, A. P. Secondary Structure and Rigidity in Model Proteins. *Soft Matter* **2013**, *9* (40), 9548.
(44) Bergfreund, J.; Bertsch, P.; Fischer, P. Adsorption of Proteins to Fluid Interfaces: Role of the Hydrophobic Subphase. *J. Colloid Interface Sci.* **2021**, *584*, 411−417.
(45) Trivedi, M. V.; Laurence, J. S.; Siahaan, T. J. The Role of Thiols and Disulfides in Protein Chemical and Physical Stability. *Curr. Protein Pept Sci.* **2009**, *10* (6), 614−625.
(46) Rahaman, T.; Vasiljevic, T.; Ramchandran, L. Conformational Changes of β-Lactoglobulin Induced by Shear, Heat, and PH—Effects on Antigenicity. *J. Dairy Sci.* **2015**, *98* (7), 4255−4265.
(47) Ma, S.; Sherwood, J. M.; Huck, W. T. S.; Balabani, S. The Microenvironment of Double Emulsions in Rectangular Microchannels. *Lab. Chip* **2015**, *15* (10), 2327−2334.
(48) Morozova, O. V.; Pavlova, E. R.; Bagrov, D. V.; Barinov, N. A.; Prusakov, K. A.; Isaeva, E. I.; Podgorsky, V. V.; Basmanov, D. V.; Klinov, D. V. Protein Nanoparticles with Ligand-Binding and Enzymatic Activities. *Int. J. Nanomedicine* **2018**, *13*, 6637−6646.
(49) Zhai, J.; Wooster, T. J.; Hoffmann, S. V.; Lee, T.-H.; Augustin, M. A.; Aguilar, M.-I. Structural Rearrangement of β-Lactoglobulin at Different Oil−Water Interfaces and Its Effect on Emulsion Stability. *Langmuir* **2011**, *27* (15), 9227−9236.
(50) Lees, J. G.; Miles, A. J.; Wien, F.; Wallace, B. A. A Reference Database for Circular Dichroism Spectroscopy Covering Fold and Secondary Structure Space. *Bioinformatics* **2006**, *22* (16), 1955−1962.
(51) Sakuno, M. M.; Matsumoto, S.; Kawai, S.; Taihei, K.; Matsumura, Y. Adsorption and Structural Change of β-Lactoglobulin at the Diacylglycerol−Water Interface. *Langmuir* **2008**, *24* (20), 11483−11488.
(52) Sakuno, M. M.; Matsumoto, S.; Kawai, S.; Taihei, K.; Matsumura, Y. Adsorption and Structural Change of β-Lactoglobulin at the Diacylglycerol−Water Interface. *Langmuir* **2008**, *24* (20), 11483−11488.
(53) Zhai, J.; Wooster, T. J.; Hoffmann, S. V.; Lee, T.-H.; Augustin, M. A.; Aguilar, M.-I. Structural Rearrangement of β-Lactoglobulin at Different Oil−Water Interfaces and Its Effect on Emulsion Stability. *Langmuir* **2011**, *27* (15), 9227−9236.
(54) Gottschalk, M.; Nilsson, H.; Roos, H.; Halle, B. Protein Self-Association in Solution: The Bovine β -Lactoglobulin Dimer and Octamer. *Protein Sci.* **2003**, *12* (11), 2404−2411.
(55) Engelhardt, K.; Lexis, M.; Gochev, G.; Konnerth, C.; Miller, R.; Willenbacher, N.; Peukert, W.; Braunschweig, B. PH Effects on the Molecular Structure of β-Lactoglobulin Modified Air−Water Interfaces and Its Impact on Foam Rheology. *Langmuir* **2013**, *29* (37), 11646−11655.

https://doi.org/10.1021/acs.biomac.2c01289
Biomacromolecules 2023, 24, 4465−4477

(56) Walstra, P.; Geurts, T. J.; Noomen, A.; Jellema, A.; van Boekel, M. A. J. S. *Dairy Technology Principles of Milk Properties and Processes*; CRC Press, 1999.
(57) Milk Proteins: From Expression to Food. In *Food Science and Technology, International Series*; Thompson, A., Boland, M., Singh, H.,, Eds.; Academic: London, 2009.
(58) Jaenicke, R. Stability and Stabilization of Globular Proteins in Solution. *J. Biotechnol.* **2000**, *79* (3), 193−203.
(59) Dai, Y.; Yang, R.; Yan, Y.; Wu, Y.; Meng, X.; Yang, A.; Wu, Z.; Shi, L.; Li, X.; Chen, H. Digestive Stability and Transport Ability Changes of β-Lactoglobulin−Catechin Complexes by M Cell Model in Vitro. *Front. Nutr.* **2022**, *9*, 955135.
(60) Barbiroli, A.; Iametti, S.; Bonomi, F. Beta-Lactoglobulin as a Model Food Protein: How to Promote, Prevent, and Exploit Its Unfolding Processes. *Molecules* **2022**, *27* (3), 1131.
(61) Ekerdt, B. L.; Segalman, R. A.; Schaffer, D. V. Spatial Organization of Celladhesive Ligands for Advanced Cell Culture. *Biotechnol J.* **2013**, *8*, 1411−1423.
(62) Cavalcanti-Adam, E. A.; Micoulet, A.; Blümmel, J.; Auernheimer, J.; Kessler, H.; Spatz, J. P. Lateral Spacing of Integrin Ligands Influences Cell Spreading and Focal Adhesion Assembly. *Eur. J. Cell Biol.* **2006**, *85* (3−4), 219−224.
(63) Deeg, J. A.; Louban, I.; Aydin, D.; Selhuber-Unkel, C.; Kessler, H.; Spatz, J. P. Impact of Local versus Global Ligand Density on Cellular Adhesion. *Nano Lett.* **2011**, *11* (4), 1469−1476.
(64) Oria, R.; Wiegand, T.; Escribano, J.; Elosegui-Artola, A.; Uriarte, J. J.; Moreno-Pulido, C.; Platzman, I.; Delcanale, P.; Albertazzi, L.; Navajas, D.; Trepat, X.; García-Aznar, J. M.; Cavalcanti-Adam, E. A.; Roca-Cusachs, P. Force Loading Explains Spatial Sensing of Ligands by Cells. *Nature* **2017**, *552* (7684), 219−224.
(65) Peng, L.; Gautrot, J. E. Growth of Mesenchymal Stem Cells at the Surface of Silicone, Mineral and Plant-Based Oils. *bioRxiv 2022.08.17.504254* **2022**, na.
(66) Abaandou, L.; Quan, D.; Shiloach, J. Affecting HEK293 Cell Growth and Production Performance by Modifying the Expression of Specific Genes. *Cells* **2021**, *10* (7), 1667.
(67) Lin, C.-Y.; Huang, Z.; Wen, W.; Wu, A.; Wang, C.; Niu, L. Enhancing Protein Expression in HEK-293 Cells by Lowering Culture Temperature. *PLoS One* **2015**, *10* (4), e0123562.
(68) Malm, M.; Saghaleyni, R.; Lundqvist, M.; Giudici, M.; Chotteau, V.; Field, R.; Varley, P. G.; Hatton, D.; Grassi, L.; Svensson, T.; Nielsen, J.; Rockberg, J. Evolution from Adherent to Suspension: Systems Biology of HEK293 Cell Line Development. *Sci. Rep.* **2020**, *10* (1), 18996.
(69) Robinson, P. J.; Bulleid, N. J. Mechanisms of Disulfide Bond Formation in Nascent Polypeptides Entering the Secretory Pathway. *Cells* **2020**, *9* (9), 1994.

https://doi.org/10.1021/acs.biomac.2c01289
Biomacromolecules 2023, 24, 4465−4477